

Structural and electrical properties of tellurovanadate glasses containing Li₂O

N. KRINS^{1,*}, A. RULMONT¹, J. GRANDJEAN², B. GILBERT³, L. LEPOT³, R.
CLOOTS¹, B. VERTRUYEN¹.

¹SUPRATECS/LCIS, Chemistry Institute B6. University of Liege, Sart-Tilman.
Liège. Belgium.

²COSM, Chemistry Institute B6. University of Liege, Sart-Tilman. Liège. Belgium.

³Analytical Chemistry and Electrochemistry, Chemistry Institute B6. University of
Liege, Sart-Tilman. Liège. Belgium.

Abstract

Glassy materials are promising intercalation compounds, due to their open network structure and absence of grain boundaries. Some glasses containing alkali ions and a high concentration of transition metal ions can present mixed ionic-electronic conductivity and are therefore potential candidates for application as cathode material in Li-ion batteries. The present work is devoted to the ternary system $x \text{Li}_2\text{O} - (1-x) [0.3\text{V}_2\text{O}_5 - 0.7 \text{TeO}_2]$ with $0 \leq x \leq 0.4$. These compounds were prepared by heat treatment in air at 800°C followed by traditional quenching. Raman spectroscopy and ⁵¹V nuclear magnetic resonance measurements were performed in order to highlight the structural short range order modifications induced by the introduction of the Li₂O network modifier. These structural effects can be related to the electrical behaviour, as studied by complex impedance spectroscopy measurements.

* Corresponding author. Tel.: +32 4 3663586; fax: +32 4 3663413.

E-mail address: nkrins@ulg.ac.be (N. Krins).

1. Introduction

Good cyclability performance is a major requirement for cathode materials in Li-ion batteries. Crystallized intercalation compounds often suffer from a lack of reversibility resulting from an irreversible phase transition when Li^+ ions are inserted in (or extracted from) the active cathode material. Glassy materials present several advantages as alternative intercalation compounds, especially (i) their isotropic structure, (ii) their open and flexible network and (iii) the absence of grain boundaries [1]. Since 20 years, many transition metal oxide (TMO) glasses have been investigated as potential cathode materials in Li-ion batteries, e.g. MoS_2 [2], V_2S_5 [2], $\text{V}_2\text{O}_5\text{-TeO}_2$ [3, 4, 5] and $\text{V}_2\text{O}_5\text{-P}_2\text{O}_5$ [4]. The binary $\text{TeO}_2\text{-V}_2\text{O}_5$ system [3, 4, 5] is particularly interesting due to its wide glass-forming region and its semiconducting properties. It also displays a good cyclability with respect to lithium intercalation in the 4 V voltage range [6]. In the present study, we have investigated the relation between structure and electrical properties in the $x \text{Li}_2\text{O} - (1-x) [0.3 \text{V}_2\text{O}_5 - 0.7 \text{TeO}_2]$ system with x ranging from 0.0 to 0.4.

2. Experimental

The lithium vanadium tellurite glass samples were prepared using the standard melt-quenching technique according to the formula $x \text{Li}_2\text{O} (1-x) (0.3 \text{V}_2\text{O}_5 - 0.7 \text{TeO}_2)$, with $0 \leq x \leq 0.4$. Appropriate amounts of V_2O_5 (99,6 % purity), TeO_2 (99.99% purity) and Li_2CO_3 (99.8% purity) were intimately mixed in an agate mortar. The mixture was then slowly heated in a platinum crucible to 800°C for 30 min. Glass powders used for structural characterisation were obtained by quenching the melt to room temperature between two brass plates, whereas disk-shaped glass samples used for the electrical characterisation were synthesized by quenching the melt in a brass mold preheated at 200°C . The resulting pellets were then annealed during 10 hours at 200°C in order to remove internal stresses and finally polished down to a thickness of $\sim 1\text{mm}$.

Glass transition temperatures (T_g) were determined by Differential Scanning Calorimetry (DSC) with a heating rate of $10^\circ\text{C}/\text{min}$.

The micro resonance Raman spectra were recorded using a LabRam spectrometer (Jobin-Yvon) provided with an Olympus confocal microscope (20 \times objective was used for simultaneous illumination and collection) and a liquid nitrogen-cooled Open-electrode 1024x256 CCD detector. An Argon-ion laser with an emission wavelength of 514.5 nm and with a power of 5 mW was used. The focal length of the spectrometer was 300 μm and the slit used was 150 μm . All measurements were integrated during 40 seconds.

Static ^{51}V NMR spectra (pulse width = 1 μs ; delay time = 5s) were recorded with 4 mm zirconia rotors on a Bruker Avance DSX 400WB spectrometer ($B_0 = 9.04 \text{T}$) working at a Larmor frequency of 105.2 MHz. The experiments were run with

700-48000 scans, depending on the paramagnetic content. The chemical shifts were referenced relative to the peak of Na_3VO_4 (= 545 ppm).

AC transport measurements were carried out between 20°C and 200°C using a Solartron 1260 Impedance Gain Phase Analyser with 0.1 Hz–10 MHz frequency range and 200 mV amplitude. Both sides of the pellets were polished and coated with gold in order to ensure good electrical contact with the gold blocking electrodes.

The temperature dependence of the DC magnetic moment was measured between 10 K and 300 K under 1 T in a Vibrating Sample Magnetometer (VSM) from Oxford Instruments.

3. Results and discussion

3.1 Electrical properties

Impedance spectra were collected for all the samples. Figure 1 shows the complex impedance plots for the samples with $x = 0.1$ and 0.4 . The spectra of all the samples present a single semi-circle at high frequency, confirming their good homogeneity [7]. In the low frequency range ($f < 10\text{Hz}$), the spectra of the samples with high Li_2O content ($x \geq 0.3$) display a straight line, characteristic of an interfacial impedance caused by the accumulation of Li^+ at the gold blocking electrode.

Figure 2 shows the influence of the Li_2O content on the total DC conductivity at 25°C and 180°C and the activation energy E_a . The E_a values were calculated by fitting the conductivity data with the equation $\sigma T = \sigma_0 \exp(-E_a/RT)$. The conductivity curves exhibit a deep minimum for an x value ranging between 0.2 and 0.3. A drastic transition in the $E_a(x)$ behaviour is observed in the same range of composition. Similar results have been reported for several transition metal oxide glasses

containing alkaline ions [8, 9, 10, 11], including the $\text{Li}_2\text{O-V}_2\text{O}_5\text{-TeO}_2$ system investigated here, but with different V/Te ratio [7, 12, 13]. Such a drastic evolution in the electrical behaviour has been attributed to the existence of two mechanisms of conduction characterized by the nature of the charge carriers. At low Li_2O content, the electronic conductivity is predominant ($0.18 \text{ eV} \leq E_a \leq 0.28 \text{ eV}$), whereas at high Li_2O content the Li^+ transport contribution becomes the most important one ($0.35 \text{ eV} \geq E_a \geq 0.32 \text{ eV}$). In the vanadium-based glass structure, the electronic transfer occurs by electron hopping along $\text{V}^{4+} \rightarrow \text{O} \rightarrow \text{V}^{5+}$ bonds and can be interpreted by the Small Polaron Model [7]. The ionic conduction path consists of a regular disposition of non-bridging oxygens (NBO's) along the network former chains, thereby allowing interstitial diffusion [7].

In order to try to understand why the electronic and ionic conductivities have opposite dependencies with respect to Li_2O content, it is necessary to study the influence of Li_2O addition on the structure of the glass network.

3.2 Structural properties

The amorphous character of the samples was confirmed by X-ray powder diffraction. The glass transition temperature (T_g) was found to decrease from 250°C to 230°C with increasing x . This confirms that Li_2O acts as a network modifier, i.e. opens the structure by creating non-bridging oxygens (NBO's).

In this amorphous system, the vanadium ions can adopt two different valence states, V^{4+} and V^{5+} , whereas the tellurium is present as Te^{4+} [3, 7, 12, 14]. V^{5+} can be either four-fold coordinated (VO_4 tetrahedron -Th) or five-fold coordinated (VO_5 trigonal bipyramid -tbp). V^{4+} cannot occupy a tetrahedral site [15, 16,17] and therefore only the five-fold coordination has to be considered in the case of V^{4+} .

Several structural units are possible for Te^{4+} ions : TeO_4 trigonal bipyramid (tbp), TeO_3 trigonal pyramid (tp) and TeO_{3+1} polyhedron (intermediate case between tbp and tp) [17,18].

The local environment of the vanadium ions has been investigated by ^{51}V NMR, magnetic measurements and Raman spectroscopy. Figure 3 shows the ^{51}V NMR spectra of each sample. In the unmodified sample ($x = 0$), V is both four- and five-fold coordinated. The addition of Li_2O leads unambiguously to a decrease of VO_5 tbp structural units in favour of an increase in VO_4 Th units. Since NMR experiments are not sensitive to the valence state of the vanadium cation, magnetic susceptibility measurements were performed in order to study the evolution of the V^{4+} content with Li_2O addition. The ratio $\text{V}^{4+}/\text{V}_{\text{TOT}}$, deduced from the paramagnetic Curie law [19], decreases from $\sim 3.6\%$ to $\sim 1.6\%$ when x increases from 0 to 0.4. These results agree with the decrease of the coordination five observed in NMR.

The micro-Raman resonant spectra are shown in Figure 4. The bands noted A, B and F are attributed to vanadium. The low-frequency bands (A and B) are assigned to V-O-V(Te) vibrations between polyhedra [20] while the F band is attributed to vibrations of V-NBO bonds ($\text{V}=\text{O} / \text{V}-\text{O}^-$) [14, 20]. The addition of Li_2O tends to shift the band A to slightly higher wavenumbers. The intensity of the B band is too small to distinguish any evolution. Addition of Li_2O shifts the band F to smaller wavenumbers.

The bands noted C, D and E are attributed to tellurium. The bands B and C are assigned to symmetric (C) and antisymmetric (D) vibrations of the Te-O-Te linkages in the TeO_4 tbp continuous network [20, 21]. The band E is attributed to the stretching vibration of Te-NBO bond present in TeO_3 tp units or in TeO_{3+1} polyhedra [20, 21]. The addition of Li_2O shifts the D and E bands to higher and smaller wavenumbers respectively.

It is observed that both bands corresponding to metal-NBO vibrations (E and F) are shifted to lower wavenumbers with increasing x. In the vanadium case, it is possible to relate this shift to the decrease of the vanadium coordination from five to four observed by ^{51}V NMR (see above) [20]. The same trend was observed by D. Bersani et al. [22] in the $\text{ZnO-V}_2\text{O}_5\text{-TeO}_2$ system. The fact that a similar shift is observed for tellurium suggests a decrease of the tellurium coordination : TeO_4 tbp units \rightarrow TeO_{3+1} polyhedra \rightarrow TeO_3 tp. Such a behaviour is consistent with the network former character of Te and V [23]. However it may be interesting to mention that Rozier et al. [15] have recently shown that an extra Li_2O addition leads to an increase in conductivity because of the restitution of V in a higher coordination.

3.3 Structure – Conductivity relationship

In the previous section, it was shown that Li_2O addition leads to significant modifications of the glass structure. These phenomena are closely linked to the transition from mainly-electronic to mainly-ionic conduction when the lithium content is increased.

Addition of Li_2O leads to an increase of the NBO concentration, a strong decrease of V^{4+} concentration and a preferential four-fold coordination of the V^{5+} ions. The increase of the NBO concentration favours the ionic conductivity. The electronic conductivity decreases due to several factors: (i) Since the electronic conductivity relies on electron hopping between V^{4+} and V^{5+} sites, the decrease of the V^{4+} concentration tends to decrease the electronic conductivity. (ii) Since V^{4+} cannot adopt a tetrahedral environment, the V^{5+} ions in tetrahedral VO_4 units cannot be involved in the hopping process. (iii) The opening of the network resulting from the creation of NBO's leads to an increase of the distance between V hopping sites.

4. Conclusions

The relationship between the structural characteristics of the $x\text{Li}_2\text{O}$ ($1-x$) ($0.3\text{V}_2\text{O}_5 - 0.7 \text{TeO}_2$) system and its electrical behaviour has been studied by Raman spectroscopy, ^{51}V NMR and impedance spectroscopy measurements. The Li-free sample ($x = 0$) presents mainly electronic conductivity resulting from electron hopping between the aliovalent sites of V (V^{4+} to V^{5+}). When increasing x , the coordination of vanadium progressively changes from five to four. The creation of non-bridging oxygens (NBO's) leads to the opening of the glassy network and results in an increase of the distance between V hopping sites. In conclusion, the addition of Li_2O in this glass system results in a decrease in electronic conductivity and an increase in ionic conductivity.

Acknowledgements

N.K. and B.V. thank the F.N.R.S. (National Fund for Scientific Research) in Belgium for research fellowships. The authors are grateful to Prof. J. Delwiche for giving them access to the VSM.

Published in Solid State Ionics 177 (2006) 3147–3150

References

1. Y. Sakurai, S. Okada, J. Yamaki and T. Okada, *J. Power Sources*, 20 (1987) 173.
2. C. Julien, *Ionics*, 2 (1996) 169.
3. M. Levy, M.J. Duclot and F. Rousseau, *J. Power Sources*, 26 (1989) 381.
4. G. Tury and M. Dawy, *Mat. Chem. Phys.*, 77 (2002) 48.
5. T. Miura and T. Kishi, *J. Power Sources*, 43-44 (1993) 645.
6. S. Jouanneau, A. Le Gal La Salle, A. Verbaera and D. Guyomard, *J. Electrochem. Soc.*, 152 (2005) A1660.
7. G.D.L.K. Jayasinghe, M.A.K.L. Diassanayake, P.W.S.K. Bandaranayake, J.L. Souquet and D. Foscallo, *Solid State Ionics*, 121 (1999) 19.
8. P. Jozwiak and J.E. Garbarczyk, *Solid State Ionics*, 176 (2005) 2163.
9. R.A. Montani, A. Lorente and M.A. Vincenzo, *Solid State Ionics*, 130 (2000) 91.
10. L. Murawski and R.J. Barczynski, *Solid State Ionics* 176 (2005) 2145.
11. H.M.M. Moawad and H. Jain, *J. Am. Ceram. Soc.*, 85 (2002) 2655.
12. E. Sanchez and C.A. Angell, *Mat. Res. Soc. Symp. Proc.*, 528 (1999) 461.
13. P. Rozier, T. Dubois and P. Salles, *J. Non-Cryst. Sol.*, 311 (2002) 241.
14. J.E. Garbarczyk., P. Machowski, M. Wasiucioneck, L. Tykarski, R. Bacewicz and A. Aleksiejuk, *Solid State Ionics*, 136 (2000) 1077.
15. P. Rozier, A. Burian and G.J. Cuello, *J. Non-Cryst. Sol.*, 351 (2005) 632.
16. R. Shannon, *Acta Cryst.*, A32 (1976) 751.
17. S. Sakida, S. Hayakawa and T. Yoko, *J. Physics: Condensed Matter.*, 12 (2000) 2579.
18. M. G. Arnaudov. and Y. B. Dimitriev, *Physical Chemistry of Glasses*, 42 (2001) 99.
19. O. Cozar, I. Ardelean, V. Simon, G. Ilonca G, C. Craciun and C. Cefan, *Journal of Alloys and Compounds*, 326 (2001) 124.
20. L. Baia, M. Bolboaca M., W. Kiefer, E.S. Yousef, C. Rüssel, F.W. Breitbarth, T. G. Mayerhöfer and J. Popp, 45 (2004) 178.
21. G.S. Murugan and Y. Ohishi, *J. Non-Cryst. Sol.*, 351 (2005) 364.

22. D. Bersani, G. Antonioli, P.P. Lottici, Y. Dimitriev, V. Dimitrov and P. Kobourova, *J. Non-Cryst. Sol.*, 232-234 (1998) 293.

23. R. N. Sinclair, A.C. Wright, B. Bachra, Y.B. Dimitriev, V.V. Dimitrov and M.G. Arnaudov, *J. Non-Cryst. Sol.*, 232-234 (1998) 38.

Figures captions

Fig. 1. Complex impedance spectra for investigated glasses with $x = 0.1$: $0.1 \text{ Li}_2\text{O} \cdot 0.9 (0.3 \text{ V}_2\text{O}_5 \cdot 0.7 \text{ TeO}_2)$ and with $x = 0.4$: $0.4 \text{ Li}_2\text{O} \cdot 0.6 (0.3 \text{ V}_2\text{O}_5 \cdot 0.7 \text{ TeO}_2)$ at 180°C .

Fig. 2. Below: total electrical conductivity as a function of the Li_2O glass content x , at 25°C and 180°C . Above: dependence of the activation energy on x .

Fig. 3. ^{51}V static NMR spectra of $x\text{Li}_2\text{O} (1-x) (0.3 \text{ V}_2\text{O}_5 - 0.7 \text{ TeO}_2)$ glasses, with $0 \leq x \leq 0.4$.

Fig. 4. Resonance micro-Raman spectra of $x\text{Li}_2\text{O} (1-x) (0.3 \text{ V}_2\text{O}_5 - 0.7 \text{ TeO}_2)$ glasses, with $0 \leq x \leq 0.4$.

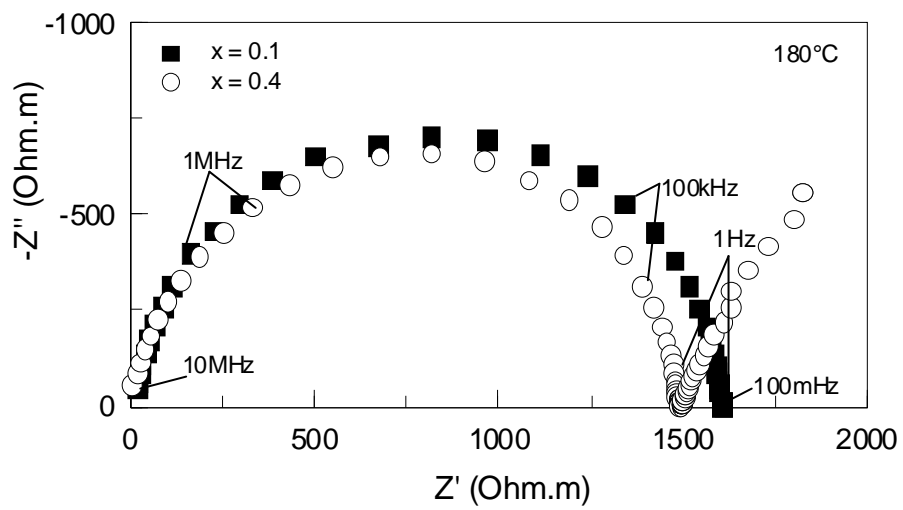


Fig. 1

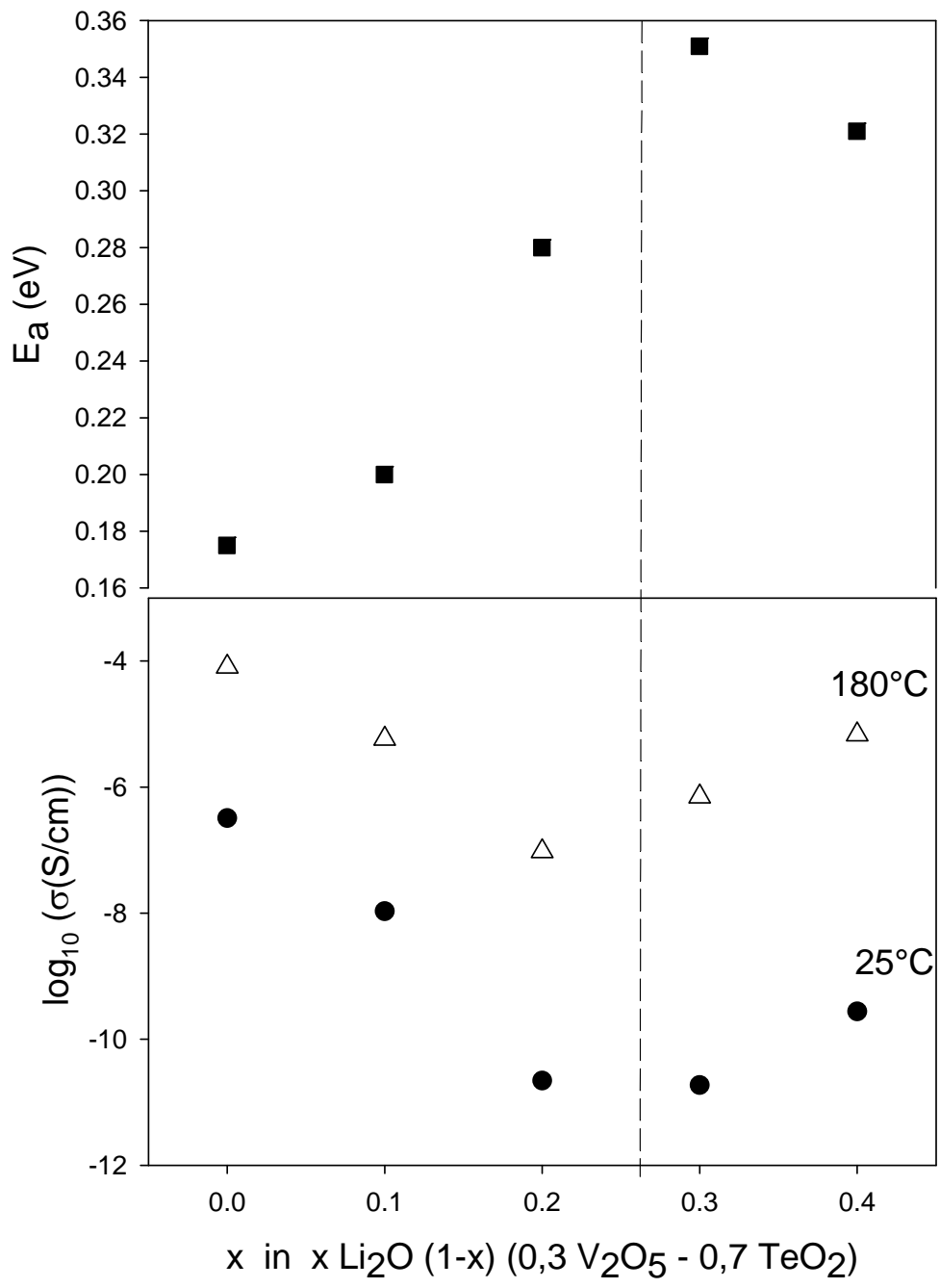


Fig. 2

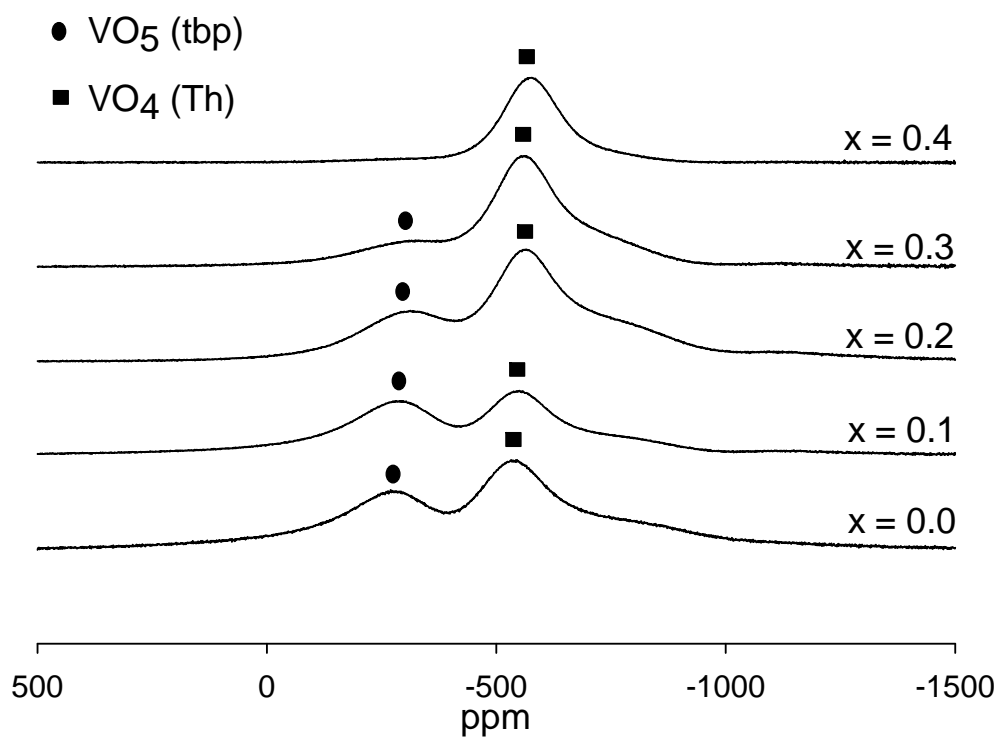


Fig. 3

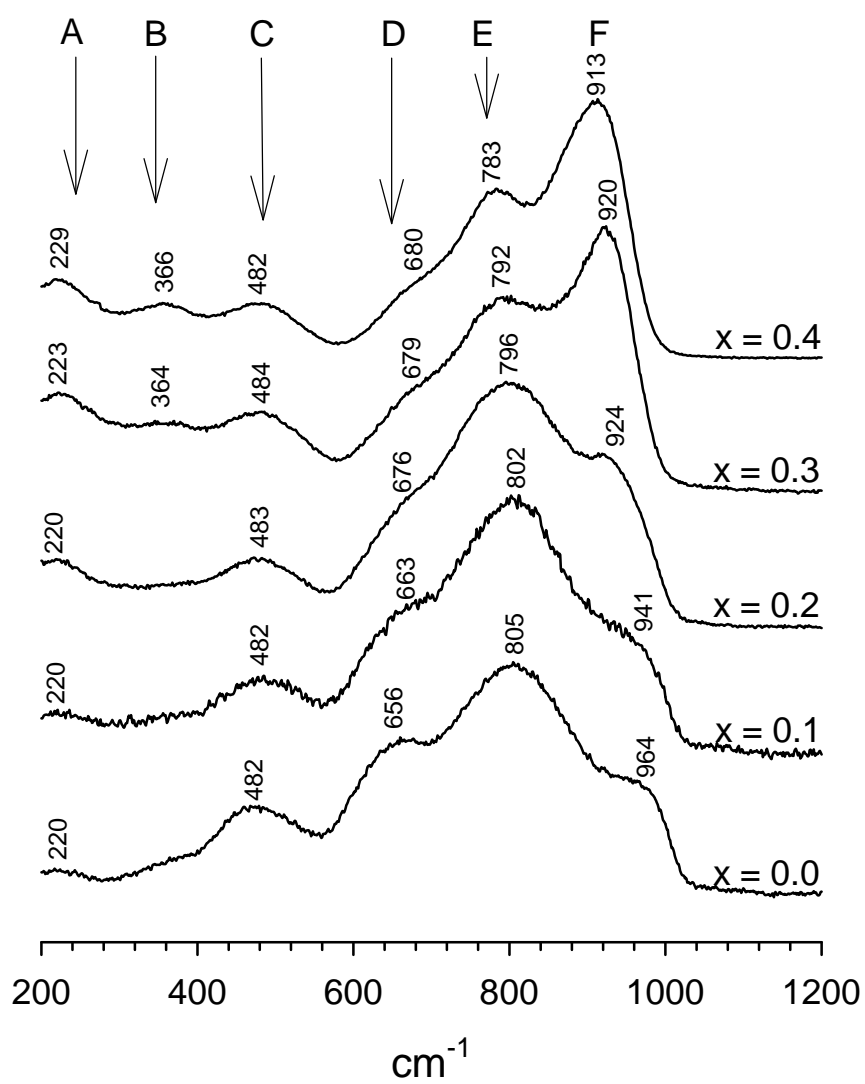


Fig. 4